

Density fluctuations at the continuous liquid-liquid phase transition in chalcogen systemsY. Kajihara,^{1,*} M. Inui,¹ K. Matsuda,² T. Nagao,² and K. Ohara³¹*Graduate School of Integrated Arts and Sciences, Hiroshima University, Higashi-Hiroshima 739-8521, Japan*²*Graduate School of Science, Kyoto University, Kyoto 606-8502, Japan*³*JASRI/SPring-8, Sayo-cho, Sayo-gun, Hyogo 679-5198, Japan*

(Received 27 January 2012; published 6 December 2012)

We have carried out density and small-angle x-ray scattering measurements on a typical liquid chalcogen (Te, Se) system to investigate its continuous liquid-liquid phase transition. With increasing temperature, the zero-wave-number structure factor $S(0)$ shows a maximum in the middle of the transition region where the density exhibits negative thermal expansion. This is direct evidence of density fluctuations induced by the liquid-liquid phase transition. When the sample is pressurized to 100 MPa, the density and $S(0)$ curves shift to the lower temperature side, which is consistent with the shift of the structural transition. We discuss the similarity between liquid Te and liquid water from the viewpoint of fluctuations induced by the liquid-liquid transition.

DOI: [10.1103/PhysRevB.86.214202](https://doi.org/10.1103/PhysRevB.86.214202)

PACS number(s): 64.70.Ja, 61.05.cf

I. INTRODUCTION

Liquid Te is known to exhibit some anomalous thermodynamics: The density is maximum^{1,2} slightly above the melting temperature (450 °C), a negative slope of the melting curve appears at high pressures,³ the heat capacity⁴ shows rapid increase in the supercooled region, and ultrasonic sound velocity^{5,6} increases with increasing temperature up to around 800 °C. To understand the origin of these thermodynamic anomalies, it is instructive to know the thermodynamics of Te-based binary liquid mixtures. In Se-Te mixtures, with increasing Se concentration, the temperature dependence of the density is gradually shifted to higher temperatures, which indicates that liquid Se-Te mixtures can be regarded as a prototype of supercooled liquid Te. Above 30%-Se concentration, it exhibits not only a maximum but also a minimum at lower temperatures^{1,7} (see also Fig. 3). In this binary liquid system, structures were investigated by neutron⁸ and x-ray⁹ diffraction measurements: They are twofold coordinated at low temperatures and/or high Se concentrations and threefold coordinated at high temperatures and/or low Se concentrations, and thus the apparent minimum and maximum densities are a consequence of a switch from the low-density to high-density state. This continuous phase transition accompanies a change in electric conductivity from semiconducting, which is typical for liquid Se, to a poor metallic, which is similar to liquid Te, state.¹⁰ On the other hand, the ultrasonic sound velocity exhibits a minimum in the middle of this phase transition,^{6,11} which reveals that this phenomenon is closely related to the phase transition. These features of the liquid Se-Te system are summarized in the phase diagram in Fig. 1. The origin of the thermodynamic anomalies of liquid Te and liquid Se-Te mixtures was discussed in the 1980s by Tsuchiya and Seymour in the framework of a two-fluid model (the inhomogeneous structure model¹²). In their scenario, large density inhomogeneity (density fluctuations¹¹) should exist in the middle of the transition region, which is the origin of the thermodynamic anomaly. The scenario is probable; however, there has been a critical problem in that no one has succeeded in the direct measurement of large density fluctuations or discrete two-fluid structures.

II. EXPERIMENTAL METHODS

To observe the density fluctuations accompanying the continuous l - l phase transition of the Se-Te system, we have carried out density and small-angle x-ray scattering (SAXS) measurements on three samples (pure Te, Se₅₀-Te₅₀, and Se₇₀-Te₃₀) at beamline BL04B2 of SPring-8 in Japan. The high-temperature (up to 1000 °C) and high-pressure (up to 100 MPa) states of the samples were achieved using tungsten heaters and by He gas compression, respectively. Samples with thicknesses of about 300–600 μm were placed in a polycrystalline sapphire cell, which was installed in a high-pressure vessel equipped with single-crystal diamond windows to allow the propagation of both incident and scattered x rays. Further details of the sample environments are given in Ref. 13. The intensities of the incident and transmitted x rays were monitored by ionization chambers and the scattered x rays were detected and accumulated for 20 min by an imaging plate (IP) of size 300 × 300 mm² located at a distance of 2.96 m from the sample position. The energy of the incident x rays was 38 keV for our preliminary measurement of liquid Se₅₀-Te₅₀¹⁴ and 62 keV for the present measurements of the three samples. The intensity of the x rays detected by the IP includes the intensity of x rays scattered from the sample, sapphire cell, and He gas, the fluorescence of Te, and the intensity of x rays multiply scattered from the sample and He gas. We estimated these values, from which we deduced the intensity of x rays scattered from the sample. The intensity was normalized by the scattering intensity of He gas as a reference, and we thus obtained the absolute value of the structure factor $S(Q)$ of each sample. Details of the data treatment will be described elsewhere.

III. RESULTS AND DISCUSSION

Figure 2 shows $S(Q)$ for liquid Se₅₀-Te₅₀ at 400, 600, and 1000 °C at 100 MPa. In the higher- Q (>5 nm⁻¹) region, $S(Q)$ changes only monotonically, but in the lower- Q region, a distinct change occurs. At both 400 and 1000 °C, $S(Q)$ in the small- Q (<3 nm⁻¹) region has almost flat Q dependence, but at 600 °C, $S(Q)$ exhibits strong Q dependence, which means that at intermediate temperatures, density fluctuations

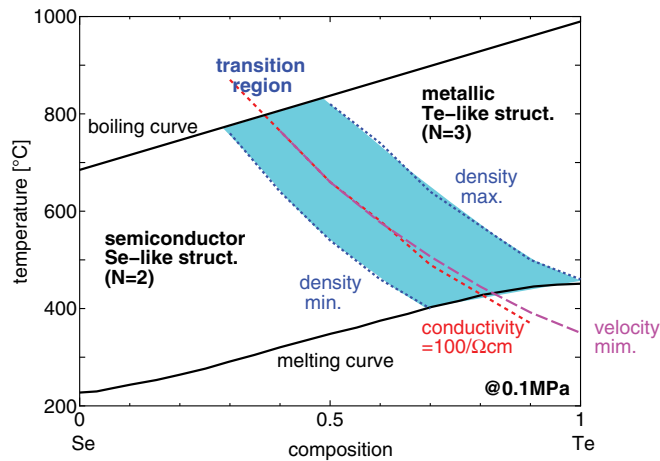


FIG. 1. (Color online) Phase diagram of Se-Te system.

of the sample increase. To clarify the situation, we fitted $S(Q)$ in the small- Q region using the linear function¹⁵ $S(Q) = S_0 - a_q Q$, shown by the dashed lines in Fig. 2. S_0 and a_q are parameters related to the intensity and size of density fluctuations, respectively.

Figure 3 shows the temperature dependence of the density and SAXS parameters (S_0 and a_q) of liquid $\text{Se}_{70}\text{-Te}_{30}$ [(a1)–(a3)], $\text{Se}_{50}\text{-Te}_{50}$ [(b1)–(b3)], and pure Te [(c1)–(c3)]. In liquid $\text{Se}_{50}\text{-Te}_{50}$, the temperature dependence of the density at 6 MPa [closed circles in Fig. 3(b1)] shows a minimum and maximum at approximately 550 and 800 °C, respectively, which is reasonably consistent with the result at ambient pressure⁷ indicated by the blue solid line. The SAXS parameters [closed circles in Figs. 3(b2) and 3(b3)], on the other hand, exhibit a broad maximum at about 650 °C, approximately midway between the temperatures at which the density exhibits a minimum and maximum. This result indicates that both the intensity and the size of density fluctuations exhibit a maximum; this is the first direct evidence of density fluctuations due to a continuous l - l transition. When the samples are pressurized

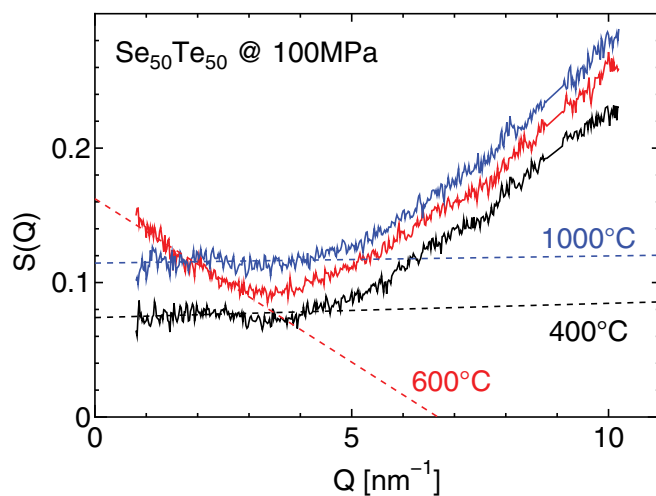


FIG. 2. (Color online) $S(Q)$ of liquid $\text{Se}_{50}\text{Te}_{50}$ at 400, 600, and 1000 °C at 100 MPa. Dashed lines are fits using a linear function in the small- Q ($< 3 \text{ nm}^{-1}$) region.

to 100 MPa, the density curve [open circles in Fig. 3(b1)] shifts to the lower-temperature side, which is consistent with the shift of the electrical conductivity¹⁶ and sound velocity curves.¹⁷ The curves of the SAXS parameters [open circles in Figs. 3(b2) and 3(b3)] also shift to the lower-temperature side and exhibit a maximum at about 600 °C, which is also in the region of the l - l transition. The intensities of both S_0 and a_q , however, decrease, which means that the density fluctuations decrease in magnitude. In $\text{Se}_{70}\text{-Te}_{30}$, the curves of the density and SAXS parameters [Figs. 3(a1)–3(a3)] shift to the higher-temperature side compared with those of $\text{Se}_{50}\text{-Te}_{50}$. These shifts are also consistent with that of the phase transition at ambient pressure (Fig. 1). The above-mentioned shifts of density and SAXS parameters with changes in pressure and concentration verify that the present density fluctuations are induced by the l - l transition. In pure Te [Fig. 3(c1)], the density at 6 MPa almost coincides with that at ambient pressure. The SAXS parameters [Figs. 3(c2) and 3(c3)] do not exhibit distinct changes in the temperature range measured. We consider that this is because the real transition region of Te is located in the supercooled region (see Fig. 1) and that the density fluctuations are too small to be detected owing to the limited experimental accuracy of our setup.

Next, we discuss the intensity of S_0 . In a pure system, the zero-wave-number structure factor $S(0)$ is related to the isothermal compressibility κ_T as $S(0) = \rho_N k_B T \kappa_T$ (ρ_N : number density, k_B : Boltzmann constant, T : temperature). In Fig. 3(c2), the value of $S(0)$ calculated from the pressure variation of the density of liquid Te¹⁸ is indicated by a pink dashed line, which almost coincides with the present value obtained by SAXS measurements plotted as closed circles. This finding verifies the validity of our estimation. Another important finding is that the absolute value of S_0 for pure Te is about 0.05 at 500 °C and 6 MPa, which is small compared with that for supercritical fluids (in the liquid-gas transition), which is usually on the order of 10^1 .¹⁹ Thus, we can conclude that the density fluctuations in the l - l transition are not sufficiently large, even though they clearly exist, to explain the large thermodynamic anomalies. We also comment on the complexity of the mixture. In a mixture, the structure factor is generally analyzed by considering three terms: the correlation between the number densities, the correlation between the concentrations of two atoms, and their cross term.²⁰ However, in this two-element mixture, there are four components: low-density and high-density species for both Se and Te. Thus, such an analysis is not appropriate at the present stage without modification.

Finally, we comment on the similarity between liquid Te and liquid water. As is well known, liquid water shows many thermodynamic anomalies:²¹ The density of liquid water is maximum at 4 °C, the melting curve has a negative slope up to about 200 MPa, the specific-heat capacity shows divergence in the supercooled region, and ultrasonic sound velocity increases with increasing temperature up to about 80 °C.²² And also, “fast sound” phenomena^{23–25} are anomalous, which is also recently confirmed for liquid Te²⁶ and liquid Se-Te mixtures.²⁷ All of these features are very similar to liquid Te; thus we believe that the origin of the anomalies is common between water and Te and parallel discussion should be instructive to understand the mechanism. Among

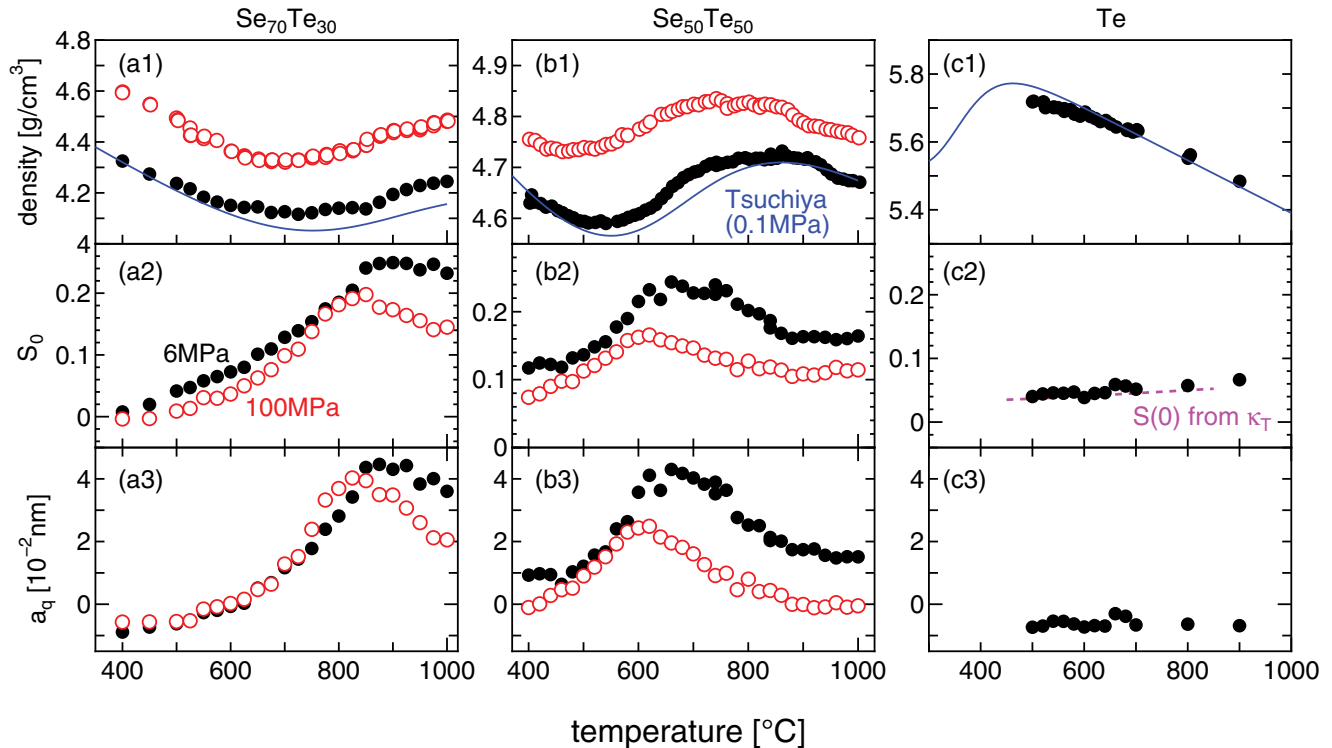


FIG. 3. (Color online) Deduced density [(a1)–(c1)] and SAXS parameters ([(a2)–(c2) S_0 and [(a3)–(c3) a_q] of liquid $\text{Se}_{70}\text{-Te}_{30}$, $\text{Se}_{50}\text{-Te}_{50}$, and pure Te. Closed and open circles denote values obtained at 6 and 100 MPa, respectively. Blue solid lines are densities at 0.1 MPa (Ref. 7). The pink dashed line shows $S(0)$ calculated from the pressure variation of the density (Ref. 18).

many scenarios for the water’s anomalies, the liquid-liquid critical point hypothesis^{28,29} is the most promising one. In water, however, it is very difficult to prove this scenario experimentally because it is impossible to access the real transition region located in the deep supercooled “no-man’s land.”²⁹ As for the fluctuations, there have been some reports^{30–34} of detecting the density fluctuations which should be the onset of the liquid-liquid transition hidden in the deep supercooled region, but there have been some criticisms of the validity and interpretation of the reported results^{35,36} mainly because the data have been limited on the high-temperature side of the transition; thus, the discussion has not yet been resolved.

In liquid Te, this problem was overcome by utilizing the Se-Te mixtures. Our experiments can hypothetically access the supercooled liquid Te and reveal the behavior of density fluctuations in the real transition region: The intensity of density fluctuations shows a maximum at around the transition temperature; with increasing pressure, the curves of density itself and density fluctuations shift to the lower-temperature side, which is consistent with the pressure variation of the density curve of liquid water.³⁷ With increasing pressure, the intensity of density fluctuations decreases, which does not contradict the pressure variation of the compressibility of liquid water.³⁸ The first two facts are also consistent with the proposed phase diagram for the liquid-liquid transition,²⁹ however, the last one seems to contradict it because it tells us that the *fluctuations* should increase in the high-pressure region. We believe that this contradiction is a very important

point for understanding the liquid-liquid transition, which differs from the liquid-gas transition.

IV. CONCLUDING REMARKS

In summary, we have carried out density and SAXS measurements on three liquid samples of the Se-Te system. The SAXS parameters exhibit a maximum at a temperature that is approximately midway through the transition where negative thermal expansion is observed. Their shifts with changes in pressure or Se concentration are consistent with that of the transition. With increasing pressure, the parameters do not increase. In the construction of a universal concept for the l - l transition, these results are significant for the following reasons: They provide clear evidence of density fluctuations accompanying the continuous l - l transition, and they reveal density fluctuations not only on the high-temperature side of the transition but also on the low-temperature side, which has not been previously observed in experiments on the liquid water system.

ACKNOWLEDGMENTS

This work was supported by Grants-in-Aid for Scientific Research from the Ministry of Education, Culture, Sports, Science, and Technology of Japan. The synchrotron radiation experiments were performed at SPring-8 with the approval of the Japan Synchrotron Radiation Research Institute (JASRI) (Proposals No. 2008B1062, No. 2009A1288, No. 2009B1583, and No. 2010A1325).

*kajihara@hiroshima-u.ac.jp

- ¹H. Thurn and J. Ruska, *J. Non-Cryst. Solids* **22**, 331 (1976).
- ²Y. Tsuchiya, *J. Phys.: Condens. Matter* **3**, 3163 (1991).
- ³B. C. Deaton and F. A. Blum, Jr., *Phys. Rev.* **137**, A1131 (1965).
- ⁴S. Takeda, H. Okazaki, and S. Tamaki, *J. Phys. Soc. Jpn.* **54**, 1890 (1985); F. Kakinuma and S. Ohno, *ibid.* **56**, 619 (1987).
- ⁵M. B. Gitis and I. G. Mikhailov, *Sov. Phys. Acoust.* **12**, 14 (1966).
- ⁶Y. Tsuchiya, *J. Phys. Soc. Jpn.* **60**, 960 (1991).
- ⁷Y. Tsuchiya, *J. Phys. Soc. Jpn.* **57**, 3851 (1988).
- ⁸R. Bellissent and G. Tourand, *J. Non-Cryst. Solids* **35-36**, 1221 (1980); S. Takeda, S. Tamaki, and Y. Waseda, *J. Phys. Soc. Jpn.* **55**, 4283 (1986).
- ⁹W. Hoyer, E. Thomas, and M. Wobst, *Z. Naturforsch.* **30a**, 1633 (1975).
- ¹⁰J. C. Perron, *Adv. Phys.* **16**, 657 (1967).
- ¹¹M. Yao, K. Suzuki, and H. Endo, *Solid State Commun.* **34**, 187 (1980).
- ¹²Y. Tsuchiya and E. F. W. Seymour, *J. Phys. C* **15**, L687 (1982).
- ¹³K. Tamura and M. Inui, *J. Phys.: Condens. Matter* **13**, 337R (2001).
- ¹⁴Y. Kajihara, M. Inui, K. Matsuda, and Y. Tomioka, *J. Phys.: Conf. Ser.* **215**, 012078 (2010).
- ¹⁵To analyze SAXS data, the Ornstein-Zernike formula is often used, but its validity has been questioned for the liquid-liquid transition (Ref. 36). Thus, we use a simpler linear function.
- ¹⁶M. Yao, M. Misonou, K. Tamura, K. Ishida, K. Tsuji, and H. Endo, *J. Phys. Soc. Jpn* **48**, 109 (1980).
- ¹⁷T. Takimoto and H. Endo, *Phys. Chem. Liq.* **12**, 141 (1982); M. Yao, N. Itokawa, H. Kohno, Y. Kajihara, and Y. Hiejima, *J. Phys.: Condens. Matter* **12**, 7323 (2000).
- ¹⁸R. Barrue and J. C. Perron, *Phil. Mag. B* **51**, 317 (1985).
- ¹⁹Y. Kajihara, M. Inui, K. Matsuda, and K. Tamura, *J. Phys.: Conf. Ser.* **98**, 012002 (2008).
- ²⁰A. B. Bhatia and D. E. Thornton, *Phys. Rev. B* **2**, 3004 (1970).
- ²¹D. Eisenberg and W. Kauzmann, *The Structure and Properties of Water* (Oxford University Press, London, 1969).
- ²²H. Tanaka, *J. Chem. Phys.* **112**, 799 (2000).
- ²³G. Ruocco and F. Sette, *Condens. Matter Phys.* **11**, 29 (2008), and references therein.
- ²⁴F. Sette, G. Ruocco, M. Krisch, C. Masciovecchio, R. Verbeni, and U. Bergmann, *Phys. Rev. Lett.* **77**, 83 (1996).
- ²⁵S. C. Santucci, D. Fioretto, L. Comez, A. Gessini, and C. Masciovecchio, *Phys. Rev. Lett.* **97**, 225701 (2006).
- ²⁶Y. Kajihara, M. Inui, S. Hosokawa, K. Matsuda, and A. Q. R. Baron, *J. Phys.: Condens. Matter* **20**, 494244 (2008).
- ²⁷Y. Kajihara *et al.* (unpublished).
- ²⁸P. H. Poole, F. Sciortino, U. Essmann, and H. E. Stanley, *Nature (London)* **360**, 324 (1992).
- ²⁹O. Mishima and H. E. Stanley, *Nature (London)* **396**, 329 (1998).
- ³⁰L. Bosio, J. Teixeira, and H. E. Stanley, *Phys. Rev. Lett.* **46**, 597 (1981).
- ³¹Y. Xie, K. F. Ludwig, Jr., G. Morales, D. E. Hare, and C. M. Sorensen, *Phys. Rev. Lett.* **71**, 2050 (1993).
- ³²C. Huang *et al.*, *Proc. Natl. Acad. Sci. USA* **106**, 15214 (2009); C. Huang, *J. Chem. Phys.* **133**, 134504 (2010).
- ³³L. Bosio, J. Teixeira, and M.-C. Bellissent-Funel, *Phys. Rev. A* **39**, 6612 (1989).
- ³⁴A. Cunsolo, F. Formisano, C. Ferrero, F. Bencivenga, and S. Finet, *J. Chem. Phys.* **131**, 194502 (2009).
- ³⁵J. C. F. Michielsen, A. Bot, and J. van der Elksen, *Phys. Rev. A* **38**, 6439 (1988).
- ³⁶G. N. I. Clark, G. L. Hura, J. Teixeira, A. Soper, and T. Head-Gordon, *Proc. Natl. Acad. Sci. USA* **107**, 14003 (2010).
- ³⁷C. A. Angell and H. Kanno, *Science* **193**, 1121 (1976).
- ³⁸H. Kanno and C. A. Angell, *J. Chem. Phys.* **70**, 4008 (1979).